
Volume 268
Issue 1
7 January 2011
ISSN 0022-5193
ELSEVIER
Journal of Theoretical Biology
50 Years

Journal of Theoretical Biology 298 (2012) 8–15

Contents lists available at SciVerse ScienceDirect

Journal of Theoretical Biology

journal homepage: www.elsevier.com/locate/yjtbi

Evolutionary dynamics of collective action when individual fitness derives from group decisions taken in the past

João A. Moreira [a], Flávio L. Pinheiro [a], Ana Nunes [b,d], Jorge M. Pacheco [a,c,*]

[a] ATP-group, CMAF, Instituto de Investigação Interdisciplinar, P-1649-003 Lisboa Codex, Portugal
[b] CFMC, Instituto de Investigação Interdisciplinar, P-1649-003 Lisboa Codex, Portugal
[c] Departamento de Matemática e Aplicações, Universidade do Minho, 4710 -057 Braga, Portugal
[d] Departamento de Física, Faculdade de Ciências, Universidade de Lisboa, Portugal

ARTICLE INFO

Article history:
Received 12 September 2011
Received in revised form
22 December 2011
Accepted 23 December 2011
Available online 8 January 2012

Keywords:
Evolutionary game theory
Delay differential equations
Evolution of collective action
Public goods games
N-Person Stag Hunt game

ABSTRACT

Many actions take some time to have an impact – their effects only appear at some point in the future. Such time lags turn out to be ubiquitous among living organisms. Here we study the impact of time lags in the evolutionary dynamics of cooperative collective action. We consider a population in which individuals interact via a N-Person Stag Hunt dilemma and must opt to cooperate or defect. In the absence of any delay, the replicator dynamics reveals the existence of regimes in which two internal fixed points appear simultaneously. We show that the presence of time delay in the fitness of individuals leads to a delayed replicator equation exhibiting new evolutionary profiles, each profile being separated by critical values of the delay that we determine explicitly. When we break the symmetry in the time lags, we show that, generally, defectors take more advantage from delay than cooperators. Finally, when we take into consideration, approximately, effects associated with the finite population size, we find that counter-intuitive evolutionary outcomes may occur, resulting from the interplay between delay and the basins of attraction in the neighborhood of the internal fixed-points, and which may lead to full cooperation in conditions under which the outcome would be Full Defection in infinite populations.

1. Introduction

More often than we would wish, the impact of our actions is not immediate, and only manifests itself in the future. There are many situations in which this happens and has a real impact on our lives: When a researcher applies for a new position, the CV that will be used to assess her/his merit by the time the evaluation panel convenes is that associated with the time of submission of the application. Economical investments made today typically generate profit only in the future. *Fernando Pessoa* or *Luís de Camões* did not live to realize they would be coined the most important Portuguese Poets. When lionesses group together to hunt for prey, their capacity to feed the community depends on food collected in the past. During winter, animals that hibernate survive by using the energy accumulated during off-winter activity. Politicians' actions take time to produce an impact. The true impact of our efforts to avoid climate change will only be felt several years in the future.

Many other examples from real life that we all have experienced or witnessed testify for the time lag that takes place between whatever we do or achieve and the impact of this achievement in our (and others) lives. Of course, the time lag associated with different actions is usually different, in some cases a few minutes, in others months, years or even centuries. Nonetheless, such time lags are ubiquitous.

Although some scholars have introduced time lags in known biological models and studied their impact (Freedman and Sree Hari Rao, 1983; Gyori and Ladas, 1991; Kuang, 1993; MacDonald, 1978), it is surprising that in the framework of evolutionary game theory such time lags have witnessed little research. In well-mixed populations interacting via symmetric two-person games, evolving according to the replicator equation, the role of time delays has been studied in the most interesting case where a mixed Evolutionarily Stable Strategy (ESS) dominates the scene in the absence of time delays. The most popular case is the *snowdrift game* (Sugden, 1986) (also known as the *chicken* or *hawk-dove* game), and this has indeed been studied by Yi and Zuwang, (1997) and also by (Alboszta and Miękisz, (2004). In a nutshell, they conclude that the presence of time delays does not change the ESS although it may render it unstable for large values of the time lag.

---

* Corresponding author at: Instituto de Investigação Interdisciplinar, ATP-group, CMAF P-1649-003 Lisboa Codex, Portugal.
Tel.: +351 21 790 4891; fax: +351 21 795 4288.
E-mail address: pacheco@cii.fc.ul.pt (J.M. Pacheco).

0022-5193/$ - see front matter © 2012 Elsevier Ltd. All rights reserved.
doi:10.1016/j.jtbi.2011.12.027

Here, we study the recent and interesting case of the N-person Stag Hunt game (NSH) (Pacheco et al., 2009b; Santos et al., 2008), where collective action takes place only whenever group participants of the public goods game coordinate to achieve cooperation. In such a setting, two internal fixed-points may arise (for a given range of the game parameters), one of which associated with a mixed ESS. The presence of more than one internal fixed point paves the way for time delays to induce non-trivial effects in the evolutionary dynamics of an infinite population. When populations are finite, not only the remnants of the internal fixed points still play a (population size dependent) role (the effect of which will be discussed) but also, in some regimes to be discussed in detail below, unexpected and counter-intuitive results are obtained. All this applies to the case in which all groups and their members experience the same time delays. Whenever the time delay is strategy-specific we find that cooperators and defectors, engaging in an NSH, are affected by time delays in fundamentally different ways.

This paper is organized as follows: In Section 2 we set the stage, revisiting the NSH game, and defining the problem in the framework of the replicator equation. In Section 3 we discuss the impact of time-lags in the evolutionary outcome of infinite populations and explore the behavior of the model in the case of finite populations. Finally, Section 4 contains the discussion of our results, the main conclusions and prospects for future studies.

2. Model

Our model considers time-delays in the NSH model introduced by Pacheco et al., (2009b); Souza et al., 2009). Suppose we have an infinite well-mixed population from which we select, at random, groups of N individuals. They are given a chance to contribute to the public good of the group, at a cost c to themselves. People who contribute are called cooperators and those that do not are called defectors. After everyone is given a chance to cooperate or defect, if the number of cooperators, k, in the group is not smaller than a given threshold M ($1 \le M < N$), the accumulated contribution is multiplied by an enhancement factor F and distributed among all the individuals of the group. The payoff of a defector is therefore $\Pi_D(k)=(kFc/N)\theta(k-M)$, whereas that of a cooperator is $\Pi_C(k)=\Pi_D(k)-c$. The presence of the threshold M is reflected in the Heaviside function $\theta\,(x)$, with $\theta\,(x<0)=0$ and $\theta\,(x \ge 0)=1$).

Let us denote by x and $1-x$ the fraction of cooperators and defectors in the population, respectively. We can compute the average fitness of each strategy using the binomial sampling of all possible payoffs associated with all possible group compositions. Thus, in a group of N individuals with k cooperators, the different strategies obtain the following average fitnesses:

$$f_D(x)=\sum_{k=0}^{N-1}\binom{N-1}{k}x^k(1-x)^{N-1-k}\Pi_D(k) \qquad (1)$$

$$f_C(x)=\sum_{k=0}^{N-1}\binom{N-1}{k}x^k(1-x)^{N-1-k}\Pi_C(k+1) \qquad (2)$$

The time evolution of the fraction of cooperators in the population is described by the replicator equation:

$$\dot{x}=x(1-x)(f_C(x)-f_D(x)) \qquad (3)$$

For a large range of parameter values, Eq. (3) has four fixed-points (see Fig. 1): Two of these correspond to the trivial monomorphic states of the population ($x=0$ and $x=1$, squares), while the two internal points, x_L and x_R ($0<x_L<x_R<1$), account for the solutions of $f_C(x)-f_D(x)=0$. The lower one (x_L, the coordination point) is unstable whereas the higher one (x_R, the coexistence point) is stable.

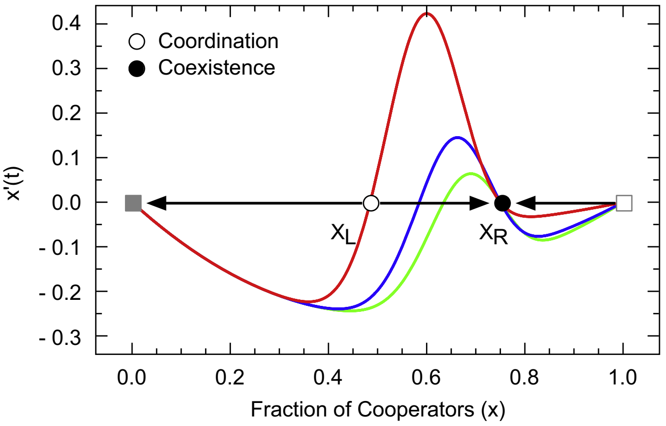

Fig. 1. Replicator dynamics for a population playing a N-Person Stag Hunt game. We study the evolutionary dynamics of the NSH for a range of parameters that leads to the existence of two internal fixed-points in the replicator equation (x_L and x_R). For simplicity, our choice of parameters (M, F and N) was such that the position of x_R remained constant at $x=0.75$, whereas x_L was shifted to obtain the desired distance δ between the internal fixed-points ($\delta=x_R-x_L$).

A quantity of interest for the present work is the distance between the two internal fixed-points, $\delta=x_R-x_L$. For convenience we kept the position of x_R constant at $x=0.75$. This allows us to vary δ by simply changing the position of x_L, as depicted in Fig. 1. Each value of δ corresponds to a triplet of game parameters: the enhancement factor (F), the level of threshold (M) and the group size (N). In order to obtain a smooth variation of δ, we worked with a modified definition of the fitnesses (Eqs. (1) and (2)) that allows for M to assume non-integer values. This does not affect the properties of the model. In the Appendix A we provide details of this transformation as well as the values of the triplets (F, M, N) associated with each value of δ used below.

To implement time delay in the model we modified Eq. (3) to make the change of frequency of cooperators at a time t depend on the average fitness the players had at a time t - τ, for some time delay τ ($\tau>0$):

$$\dot{x}=x(t)(1-x(t))\left[f_C(x(t-\tau))-f_D(x(t-\tau))\right] \qquad (4)$$

This equation corresponds to the standard (Alboszta and Miękisz, 2004; Yi and Zuwang, 1997) (and simplest) case of *symmetric delay*, in which every strategy has the same time delay between change and fitness driving such change. Note that the existence and location of the fixed-points is unchanged by τ. Below we show that the introduction of this time lag modifies the stability of the coexistence point. In fact, there is a critical value of τ, τ_C, at which a Hopf bifurcation occurs, leading to a change from a stable to an unstable behavior, accompanied by the emergence of periodic solutions.

More general, less symmetric formulations of time delays can be made. For instance, delays may be strategy dependent:

$$\dot{x}=x(t)(1-x(t))\left[f_C(x(t-\tau^C))-f_D(x(t-\tau^D))\right] \qquad (5)$$

In this manuscript we consider the formulations of Eqs. (4) and (5). Moreover, in the case of Eq. (5), we shall consider that only one of the two possible delays τ^C, τ^D, is different from zero. For these two cases, the Hopf bifurcation line of the coexistence equilibrium can be found analytically (Kuang, 1993). Apart from this technical advantage, the cases we will explore were chosen because they illustrate the two opposite extremes concerning the general behavior, namely the maximally symmetric ($\tau^C-\tau^D=0$) and the maximally asymmetric ($\tau^C\tau^D=0$) choice for the delays associated with each strategy.

A problem that arises when dealing with delay differential equations (DDE's) is the choice of the so-called *history function* of the system, i.e., the (infinite dimensional) initial condition that defines how x evolved during the time interval $[-\tau, 0]$. This choice does not influence the stability properties of the coexistence point. However it can have a significant impact in the evolutionary outcome of the population, as we demonstrate below.

In this manuscript we focus our study on the impact of time delays in the evolutionary dynamics of a population that at time $t=0$ is composed by a fraction x_R of cooperators. To that end, we take as history function a perturbation such that the population composition is set on x_R both at $t=-\tau$ and $t=0$ and it oscillates with a small amplitude around this value from $t=-\tau$ to $t=0$. The choice of this history function corresponds to the idea that, before the delay sets in, the population undergoes small fluctuations around the stable coexistence equilibrium point. We will make use of two variations of this history function to account for the effect of increasing or decreasing the fraction of cooperators at $t=-\tau$, which we found to be relevant. Consequently, we shall start the first oscillation with an increasing or decreasing behavior from x_R, respectively. The history function is described in full detail in the Appendix B, where we also consider the standard choice of a homogeneous history function. Overall, the nature of the results does not depend on the specific choice made for the history function.

Needless to say, other history functions are possible. However, these often require additional parameters that directly influence the evolution of the population and whose analysis presents, by itself, an additional layer of complexity.

3. Results

3.1. Symmetric case: A common time delay

The stability of the coexistence point (x_R) for the delayed system, as described by Eq. (4), can be obtained from the analysis of the linearized equation at x_R,

$$\dot{x} = ax(t-\tau) \tag{6}$$

where $a=x^*(1-x^*)(f'_C(x^*)-f'_D(x^*))$ and $x^*=x_R$ is the frequency of cooperators at the coexistence point. The characteristic equation of (6) reads (Kuang, 1993)

$$\lambda - ae^{-\lambda\tau} = 0 \tag{7}$$

The roots of Eq. (7) are given by

$$\lambda = W(a\tau)/\tau \tag{8}$$

where W is the Lambert function (Kuang, 1993). The Hopf bifurcation at the coexistence point takes place when the real part of the principal branch $W(a\tau)$ in Eq. (8) goes through zero and reads $\tau_C = -\pi/2a$.

To go beyond linear stability analysis and to study the behavior of the population for larger values of τ one must resort to numerical integration. In Fig. 2 we show three integrations of Eq. (4) over time for three different delays ($\tau=0.5$, 1.0 and 2.0) and the same $\delta=0.15$.

The integration of Eq. (4) gives rise to three distinct evolutionary behaviors: For small delays the dynamics of the population remains unchanged and the population is driven to a stable coexistence – this is what we call Phase I. Above a critical delay, τ_C, which corresponds to the Hopf bifurcation at the coexistence point, we enter what we call Phase II, in which the stability of x_R changes and a stable periodic orbit appears. Thus the population will be trapped on periodic oscillations around x_R. As we increase the delay, so does the amplitude of the periodic orbit. For sufficiently large delays, the amplitude will be large enough to bridge the distance δ and reach x_L. At this point the periodic orbit disappears or becomes unstable, so that the population will be driven to Full Defection, entering what we call Phase III. These three behaviors are depicted in Fig. 2.

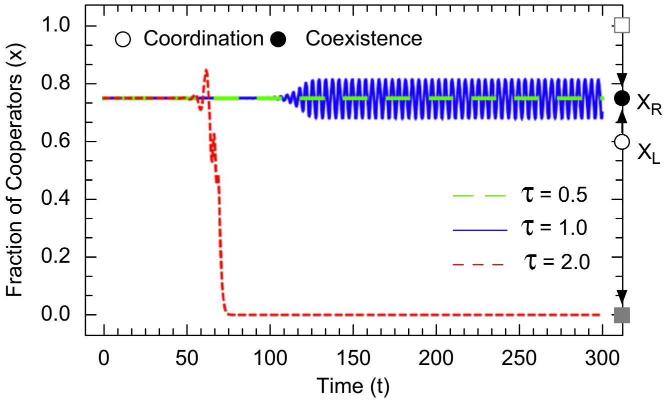

Fig. 2. Examples of time integrations and associated behavior The game parameters are: $M=26.9831$, $F=14.9419$ and $N=40$ which correspond to $\delta=0.15$. Each integration uses a different value for the time delay τ (indicated) leading to different behaviors. On the right hand side of the plot, we characterize the nature of the fixed points of the corresponding evolutionary dynamics in the absence of delay.

In both Phase I and II the evolutionary outcome is qualitatively identical to the one expected before the introduction of delay, in the sense that although the dynamics are different the population is always composed of a mixed amount of both strategies. However, in Phase III we observe a different evolutionary outcome as the population is always driven to Full Defection.

More important than τ_C which, as discussed above, defines the boundary between Phase I and Phase II and can be found analytically, there must exist for each δ an additional critical delay, τ'_C, above which the population will asymptotically end up in Full Defection. In other words, this τ'_C defines another boundary, between Phases I and II, characterized by strategy coexistence, and Phase III, characterized by Full Defection.

Fig. 3 shows the bifurcation diagram of Eq. (4) as a function of the parameters τ and δ. The results were obtained by numerical integration of Eq. (4) with a history function that corresponds to a small perturbation around x_R. Overall, the contour plot is the result of over 12,000 integrations. The analytical prediction for τ_C is shown to fit perfectly with the numerical integration illustrating the accuracy of the numerical phase diagram. In Fig. 3 we also depict the behavior of τ'_C.

Finally, it is noteworthy that the persistence, as the delay τ increases, of the stable periodic orbit O, associated with Phase II, depends strongly on the position of the internal fixed points x_L and x_R, given here by the parameter δ. This can be understood if we think that O must live in the basin of attraction of x_R, for $\tau=0$, and that its amplitude increases with τ[1] asymmetrically, reflecting the existing asymmetry of $\dot{x}(t)$ around x_R (see Fig. 1), so that the minimum of $x(t)$ along O approaches x_L faster than the maximum approaches $x=1$. The breakdown of the stable oscillations associated with O takes place when the troughs of $x(t)$ along O cross x_L. For small values of δ this happens for small amplitudes of O and small values of τ, which results in a relatively thin Phase II. For larger values of δ the area associated with Phase II increases significantly,

---

[1] This is because the oscillations of O around x_R reflect the delayed effect of the change in sign of the derivative $\dot{x}(t)$ as x crosses x_R in the basin of attraction bounded by x_L to the left and by $x=1$ to the right, see Fig. 1.

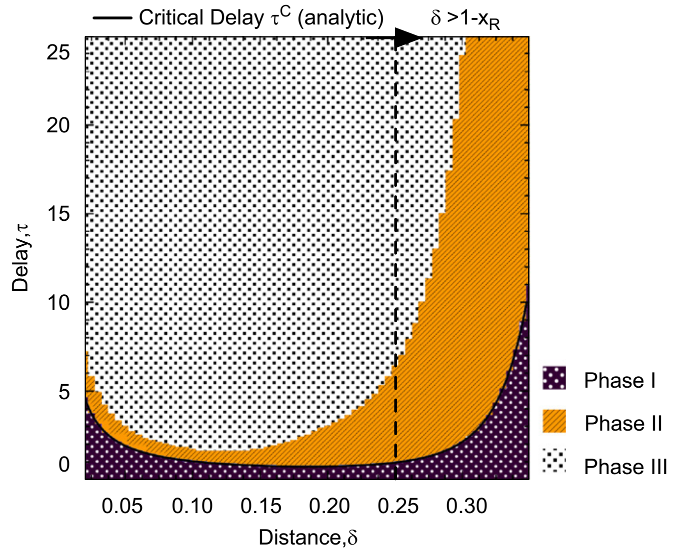

Fig. 3. Bifurcation diagram of the delayed N-Person Stag Hunt dynamics. We identify three phases associated with the evolutionary dynamics of the population: in Phase I, the population is driven to the coexistence point as the dynamics remains unchanged by the delay (illustrated by the long-dashed line in Fig. 2); in Phase II we are above the Critical Delay and thus the system oscillates periodically around x_R (illustrated by the solid line in Fig. 2); finally in Phase III oscillations are broken by the influence of the coordination point x_L, which pushes the population to a Full Defection scenario (short-dashed line in Fig. 2).

becoming the dominant behavior whenever $\delta > 1-x_R$. In other words, when the distance between the fixed-points is greater than that between the coexistence point and $x=1$.

3.2. Asymmetric case: strategy-specific delays

Let us consider now the case of asymmetric delays, in which case, as stated before, we set either τ^C or τ^D to zero in Eq. (5). The linearized equation at x_R has now the form

$$\dot{x} = ax(t-\tau)+bx \tag{9}$$

where $a=-x^*(1-x^*)f'_D(x^*)$ and $b=x^*(1-x^*)f'_C(x^*)$ when $\tau^C=0$, and $a=x^*(1-x^*)f'_C(x^*)$ and $b=-x^*(1-x^*)f'_D(x^*)$ when $\tau^D=0$. The characteristic equation of (9) is (Kuang, 1993):

$$\lambda - ae^{-\lambda\tau} - b = 0 \tag{10}$$

and the roots of (10) are given by

$$\lambda = b + W(a\tau e^{-b\tau})/\tau \tag{11}$$

When $\tau^D=0$, $a>0$, $b<$ -a and λ, given by (11), is real and negative for every τ. In other words, the coexistence point becomes less stable as the delay τ increases, but its stability type is left unchanged by the introduction of arbitrarily large delays.

When $\tau^C=0$, the effect of the delay is similar to the symmetric case, although less pronounced. In Fig. 4 we plot the bifurcation diagram of Eq. (5) as a function of δ and $\tau^D=\tau$. Similar to Fig. 3, in Fig. 4 we identify the same three Phases. The evolutionary outcome of cooperation under this new scheme of delays is characterized by a near absence of Phase II and by the relatively low (when compared with the symmetric delay scheme) critical delays above which the population ends in Full Defection. The range of parameters for which cooperation is sustainable is significantly reduced in this case. Clearly, defectors benefit more from delays than cooperators.

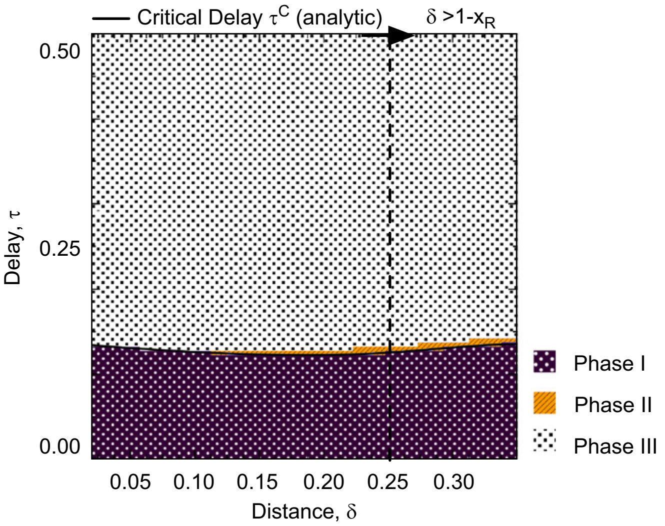

Fig. 4. Bifurcation diagram for Asymmetric delays. The plot shows the bifurcation diagram for a delayed NSH game where only the defectors experience a delayed fitness. This asymmetric case is characterized by the near absence of a Phase II and an almost constant τ_C (in comparison with Fig. 3). When only the defectors are affected by the delay, their chances increase in comparison to the symmetric case shown in Fig. 3.

3.3. Finite population-size effects

So far we have not taken into consideration that the possibility of an orbit getting arbitrarily close to $x=1$ (the fully cooperative scenario) is an artifact of the infinite population ansatz we are employing. In real situations, populations are finite and the population is bound to spend a finite amount of time in the vicinity of $x=1$.

To account for population finite-size effects, we define a cut-off value of $x_{\mathrm{cutoff}}=1-\ 10^{-3}$ taking x to be effectively one whenever it goes above this value during the numerical integrations (this implicitly assumes a population of 1000 individuals; note further that, in an actual finite system, expressions (1) and (2) for the calculation of the average fitness should, in full rigor, be replaced by sampling without replacement) (Międzisz and Wesołowski, 2011).

We consider Eq. (4) in this approximate scheme using variations of the history function which take into account whether x starts, at $t=-\tau$, by increasing (left panel of Fig. 5) or decreasing (right panel of Fig. 5).

Two distinct types of behavior can lead a population to go over the cutoff. The first is when the parameters (δ and τ) create an orbit O whose amplitude takes x over x_{cutoff}. This behavior is independent of the history function and we call this type of "*fixation*" Type I. A second behavior – Type II – depends on the initial conditions. It occurs for parameter values for which the stable orbit O is below x_{cutoff} and it is associated with orbits that may reach the cutoff in the transient *before* they are attracted to O, typically in the first or second swings of $x(t)$. The transient is strongly dependent on the history function, and so is the region associated with this behavior. Examples and further discussion are deferred to Appendix C.

In Fig. 5 we show the region of parameters that give rise to both Types of fixation. Note that the Type II fixation is sensitive to the history function variation that we use, and thus constitutes a less robust type of fixation. The overall picture can be understood in terms of the relation between the stable periodic orbit O and the basin of attraction of x_R, as discussed above for the infinite population limit. Type I fixation is independent of the initial conditions but it is confined to Phase II and mostly restricted to

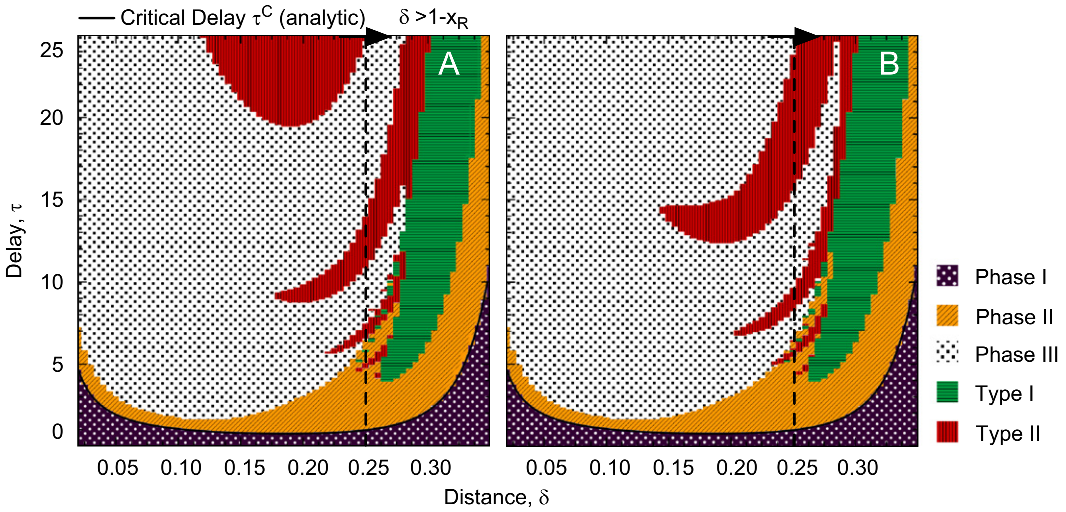

Fig. 5. Finite size effects in the evolutionary outcome of a delayed NSH game. We define two types of behavior that lead to different fixation scenarios, which we denote by Type I and Type II. In Type I, the population is able to reach fixation independently of the history function, as values above the cutoff ($x_{\text{cutoff}}=1-10^{-3}$) are attained along the periodic oscillations. In Type II fixation, the population only reaches above x_{cutoff} once, in a first stage that is otherwise not reflected in the evolutionary outcome of the game. In pannel *A*, x increases at the start ($t=-\tau$) whereas in pannel *B* it decreases at the start. In all cases, a symmetric delay was considered.

the region $\delta>0.25$, which is in accordance with the previous discussion in Section 3.1. Type II fixation can occur both in Phase II and in Phase III, and while in Section 3.1 we presented Phase III as a situation in which the population is always led to Full Defection, for finite populations we observe a coordination dynamics where the population, depending on the initial fraction of cooperators (in relation to x_L), either fixates in Full Cooperation or in Full Defection.

Therefore, and counter-intuitively, specific conditions, which may depend on the history function, may drive a finite population into a *Full Cooperation* scenario both in Phase II and in Phase III. The chances that the population fixates in full cooperation increase for increasing δ and increasing delays. For asymmetric delay, fixation is characterized by the absence of Type I fixation and, consequently, by a more explicit dependence on the initial conditions (see Appendix D).

4. Discussion

In this work we have introduced both symmetric and asymmetric delays into NSH evolutionary games. Three distinct evolutionary outcomes were identified, as depicted in Fig. 2, which depend on the magnitude of delay τ and on the distance δ between the internal fixed-points of the NSH. A critical delay, corresponding to the value at which we find a Hopf bifurcation at the coexistence point, can be computed analytically. Above this delay the population dynamics is dominated by oscillations around the coexistence point. Numerical exploration of the system led us to identify yet another critical delay, above which the population ends in Full Defection. In Fig. 3 and Fig. 4 we plot the bifurcation diagrams of the population dynamics with symmetric and asymmetric delays, respectively.

Recently, we have shown that the simultaneous appearance of 2 internal fixed points in the evolutionary dynamics of populations is ubiquitous in Biological and Social Sciences (Pacheco et al., 2009c; Santos and Pacheco, 2011; Souza et al., 2009). Furthermore, this feature arises not only as a result of individuals engaging in threshold public goods games, but also when individuals engage in two-person games along the links of complex networks which, together with the game at stake, ultimately dictate the detailed interplay and location of the internal fixed points. In this sense, our results for infinite populations and symmetric or asymmetric delays suggest that delays not only de-stabilize the stable equilibrium but also, overall, favor defection. Once again, and remarkably, such a ubiquitous feature of any biological systems – time delay – seems to reinforce the grim message from standard Evolutionary Game Theory – defection is evolutionary advantageous.

In Section 3.3, however, we inspected finite population-size effects for symmetric delay. In this case, which is more realistic from a biological perspective, we showed how the dynamics is enriched as a result of finite population-size effects. The results (Fig. 5) show that the evolutionary outcome of the population is strongly dependent on its past. In particular, appropriate choices of history functions may, in principle, drive the population into all possible outcomes, giving delay and non-markovian effects a central role to play in the evolutionary dynamics of populations.

From a wider perspective, delayed fitnesses provide the population with the ability to leave the basin of attraction of the mixed ESS, in favor of others (e.g. Phase III). Indeed, in Phase II, coexistence is characterized by stable periodic oscillations around a mixed ESS. For a large range of the parameters considered, characterized mostly by low enhancements and high threshold levels, small delays are enough to switch from coexistence of strategies to irreversible demise of cooperators (small Phase I and II); as enhancements are increased and thresholds decreased, the distance between the internal fixed points becomes larger, creating a more favorable setting for cooperation, which now becomes protected from increasing delays, (large Phase II). In particular, for finite populations this widening of Phase II is accompanied by a chance for cooperators to invade the entire population (Type I and II behavior). From an evolutionary perspective, it is reasonable to assume that, long time ago, populations were small, the same happening with thresholds, while the returns from successful coordination were potentially very high. In others words, it is conceivable that early in evolution conditions were ripe for cooperation to thrive. As populations grew as well as their organizational complexity, it is possible that the evolutionary dynamics has enabled populations to maintain cooperation as a viable evolutionary outcome.

This work investigated the simplest scenarios that arise as a result of introducing delays in the population dynamics of collective action. In this sense, they should be considered as a first step toward further studies on the impact of delay in the evolutionary dynamics of collective action. Steps ahead include investigating explicitly the role of delay in finite populations, in a manner similar to, e.g., (Miękisz and Wesołowski, 2011), as well as in structured populations (Nowak and May, 1992; Santos et al., 2006; Szabo and Fath, 2007), given their importance in relating evolutionary game theory models and real population dynamics. Furthermore, given that recent studies positively correlate social diversity (McNamara et al., 2004; Pacheco et al., 2009a; Perc and Szolnoki, 2008; Santos and Pacheco, 2005; Santos et al., 2008; Santos et al., 2011; Van Segbroeck et al., 2009) with the sustainability of cooperation, it is only natural to investigate the role of diversity of delays into the evolutionary dynamics of collective action. Work along these lines is in progress.

Acknowledgments

Financial support from FCT Portugal is gratefully acknowledged. The authors would like to thank Carlos L. Reis for help in choosing and implementing suitable integration routines for delayed differential equations.

Appendix A. Game parameters and fitness functions

From (Pacheco et al., 2009b) we know that any internal fixed-point of the replicator equation of the NSH with threshold satisfy:

$$f_c(x) - f_d(x) = -c\left[1 - \frac{F}{N}R(x)\right] \tag{A.12}$$

Assuming that we have a pair of fixed-points, x_L and x_R, for a set of game parameters (M, F and N) then the following applies:

$$R(x_L) = R(x_R) = N/F \tag{A.13}$$

As discussed in the manuscript, the relevant parameter of interest for this work is the distance (δ) between x_R and x_L. To be able to treat δ as a continuous parameter we re-define the polynomial $R(x)$ as:

$$R(x) = I_k(M, N-M) + M\frac{\Gamma(N)}{\Gamma(M)\Gamma(N-M+1)}x^{M-1}(1-x)^{N-M} \tag{A.14}$$

where Γ is the gamma function, the generalization of the factorial to real numbers, and I_k is the regularized beta function

$$I_k(a,b) = \frac{B(x;a,b)}{B(a,b)} \tag{A.15}$$

with $B(x;a,b)$ the incomplete beta function:

$$B(x;a,b) = \int_0^x t^{a-1}(1-t)^{b-1}\,dt \tag{A.16}$$

and $B(a,b)$ the beta function (Eq. (A.5) with $x=1$). Whenever a and b are integers I_k simplifies to

$$I_k(a,b) = \sum\nolimits_{j=a}^{a+b+1} \frac{(a+b-1)!}{j!(a+b-1-j)!}x^j(1-x)^{a+b-1-j} \tag{A.17}$$

in which case Eq. (A.3) reduces to the $R(x)$ of (Pacheco et al., 2009b). Hence, using I_k we can nicely expand our studies to real F and M: for given N, x_L and x_R, we can compute, from the first equality of (A.2) and through numerical methods, a value of M; then, from the last equality of (A.2), we determine the corresponding F.

The parameters were computed taking x_R fixed at 0.75 and $N=40$. In Table A1 we provide all the game parameters (M, F and N) used for each value of δ.

Table A.1
Game parameters leading to a constant x_R. The integrations on Sections 3 and 4 of the main work were carried out using the combination of parameters tabulated. The columns are, from left to right: the value of δ;N stands for the group size; M defines the threshold parameter; F corresponds to the enhancement factor of the game; x_L gives the position of the coordination point; δ the distance between the coexistence point (x_R) and the coordination (x_L) point: $\delta = x_R - x_L$.

δ	x_L	N	M	F
0.020	0.730	40	29.60152029	8.593394007
0.025	0.725	40	29.50227975	8.685166955
0.030	0.720	40	29.40313568	8.786696175
0.035	0.715	40	29.30406265	8.898130145
0.040	0.710	40	29.20505209	9.019625394
0.045	0.705	40	29.10606634	9.15140071
0.050	0.700	40	29.00708018	9.293689767
0.055	0.695	40	28.90807249	9.446747352
0.060	0.690	40	28.80902236	9.610853205
0.065	0.685	40	28.7098938	9.786339079
0.070	0.680	40	28.61066669	9.973536598
0.075	0.675	40	28.511308	10.17282663
0.080	0.670	40	28.41179125	10.38460364
0.085	0.665	40	28.31208407	10.60929947
0.090	0.660	40	28.21217183	10.84732791
0.095	0.655	40	28.1120014	11.09921679
0.100	0.650	40	28.01154721	11.36545224
0.105	0.645	40	27.91078711	11.64652698
0.110	0.640	40	27.80966702	11.94304116
0.115	0.635	40	27.70816147	12.25553137
0.120	0.630	40	27.60622489	12.58460691
0.125	0.625	40	27.50381772	12.93086999
0.130	0.620	40	27.40090164	13.294923
0.135	0.615	40	27.29742468	13.67741745
0.140	0.610	40	27.19333165	14.07901637
0.145	0.605	40	27.08859316	14.50026921
0.150	0.600	40	26.9831347	14.94188315
0.155	0.595	40	26.87690583	15.40444187
0.160	0.590	40	26.76984107	15.88855186
0.165	0.585	40	26.66187464	16.3947692
0.170	0.580	40	26.55294692	16.92354993
0.175	0.575	40	26.44297009	17.47540001
0.180	0.570	40	26.33186743	18.05066874
0.185	0.565	40	26.21956061	18.64958285
0.190	0.560	40	26.10595213	19.27231697
0.195	0.555	40	25.99094618	19.91885754
0.200	0.550	40	25.87443483	20.58904754
0.205	0.545	40	25.75631426	21.28246086
0.210	0.540	40	25.63646391	21.99848693
0.215	0.535	40	25.51475299	22.736259
0.220	0.530	40	25.39105158	23.49454805
0.225	0.525	40	25.26521139	24.2718418
0.230	0.520	40	25.13708745	25.06617547
0.235	0.515	40	25.00652161	25.87520128
0.240	0.510	40	24.87334085	26.69617327
0.245	0.505	40	24.73737953	27.52579436
0.250	0.500	40	24.59846488	28.36030653
0.255	0.495	40	24.45639843	29.19561576
0.260	0.490	40	24.31101104	30.0270045
0.265	0.485	40	24.16211792	30.84946873
0.270	0.480	40	24.00954664	31.65765429
0.275	0.475	40	23.85312517	32.44605509
0.280	0.470	40	23.69271507	33.20901103
0.285	0.465	40	23.52818201	33.94105575
0.290	0.460	40	23.35942702	34.63698227
0.295	0.455	40	23.18638398	35.29209041
0.300	0.450	40	23.00902981	35.9023713
0.305	0.445	40	22.82737268	36.4647426
0.310	0.440	40	22.64147598	36.97711481
0.315	0.435	40	22.45145785	37.43849596
0.320	0.430	40	22.25745936	37.84908298
0.325	0.425	40	22.05967719	38.21011615
0.330	0.420	40	21.85833222	38.52382096
0.335	0.415	40	21.65368716	38.79319634
0.340	0.410	40	21.44598597	39.02188181
0.345	0.405	40	21.23552339	39.21384367
0.350	0.400	40	21.02255328	39.37326291

Appendix B. History function

The history function we used corresponds to a small amplitude oscillation around the coexistence point, x_R, in the time interval $[-\tau\ , 0]$. It is defined in such a way that, at the extremes of the interval ($t=-\tau$ and $t=0$), the population is composed of a fraction x_R of cooperators. Thus the history function is:

$$A\sin(Bt/\tau)+x_R \quad \text{(B.1)}$$

where A defines the amplitude, $|B|$ the frequency and the sign of B the initial phase of the oscillation.

The impact of these two parameters in the evolutionary dynamics is different but it is relevant only for the finite population model discussed in Section 3.3 because the stability properties of the fixed points are independent of the history function (Kuang, 1993).

In Figs. 3, 4 and 5 we used $A=10^{-10}$ and $B=1$. In Fig. B.1 we fixed δ to illustrate the influence of the parameters A and B on the behavior of the system.

In Section 3.3, where finite populations are discussed, the impact of the sign of B was taken into account by considering $B=1$ and $B=-1$, meaning that the first oscillation starts increasing or decreasing from x_R, respectively.

For the sake of completeness, we have also considered the homogeneous history functions $x(t)=x_R$, in the time interval $[-\tau,0)$, and $x(\tau)=A$ or $x(\tau)=-A$. For infinite population size, the results remain unchanged. We obtain again the numerical phase diagrams of Figs. 3 and 4, consistent with the attractors associated with each phase being global attractors for the system. The results for finite population size are slightly changed in what concerns Type II fixation. This is to be expected since Type II fixation depends on the initial condition through the corresponding transient. For the homogeneous history functions with and $x(\tau)=A$ and $x(\tau)=-A$ we obtain a behavior similar to that depicted in the right and left panels of Fig. 5, respectively. The only difference is that the parameter region of Type II fixation becomes slightly smaller, and the region of global defection slightly larger, for the case of homogeneous history functions.

Appendix C. Fixation Types (symmetric delay)

In Section 3.2 we classified two types of behaviors that lead the population to fixation by 'artificially' setting $x=1$ when x goes above the imposed cut-off of $x_{\text{cutoff}}=1-10^{-3}$. This is the simplest way to simulate a finite population within our approach.

In Fig. C.1 we show two trajectories for the same δ and history function ($A=10^{-10}$ and $B=1$) but for two different values of delay. In the trajectory of Type I (left panel), the system repeatedly goes above x_{cutoff}, because it does so as it follows the periodic orbit O. By contrast, in the trajectory of Type II (right panel) this only happens in the transient stage which precedes the convergence to O that we call Stage I. In the particular case illustrated in Fig. C.1, the system goes above the cut-off only once during Stage I after which it oscillates around x_R following O (Stage II) without

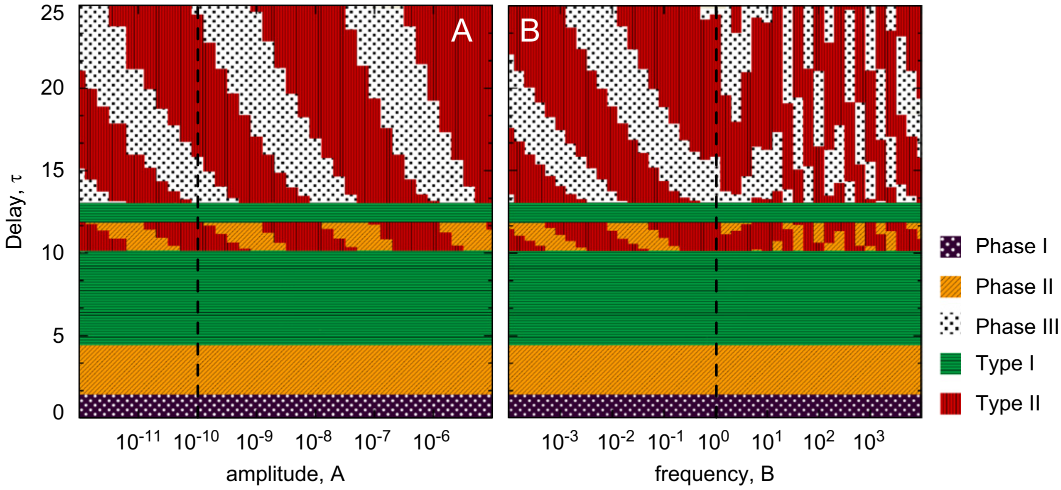

Fig. B.1. Bifurcation diagram for Symmetric delays and different history function parameters. Setting $\delta=0.28$ and fixing $A=10^{-10}$ and $B=1$, on the right and left panels, respectively, we study the effect of the history function parameters A and B on the different behavioral regions of the system. As expected, the three Phases have the same size and shape on both panels as well as the Type I fixation. The two panels coincide on the dotted line (equal A and B).

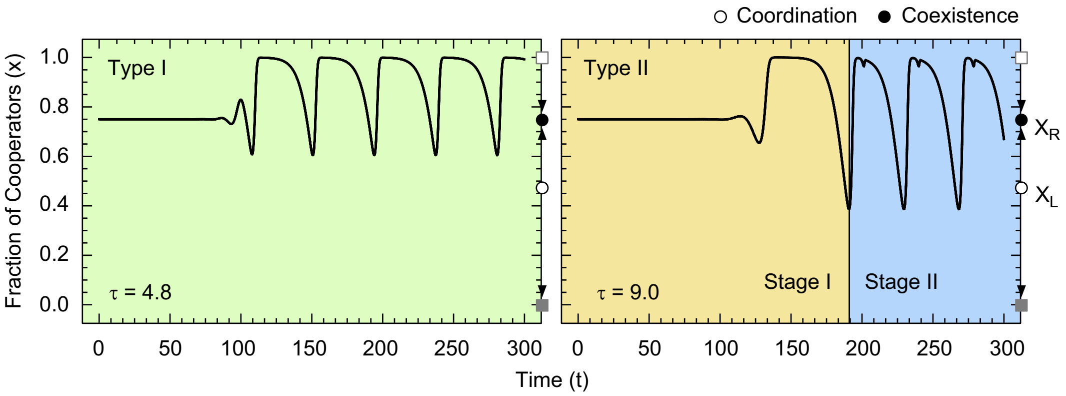

Fig. C.1. Types of Orbits and different behavioral regions. The 2 orbits were computed for $\delta=0.275$ and using a history function with $A=10^{-10}$ and $B=1$. For different delays (left and right panel) we observe two different types of fixation (Type I and Type II): in the first example (left) the population periodically crosses x_{cutoff}; while in the second example (right) the population only crosses this value once, in Stage I.

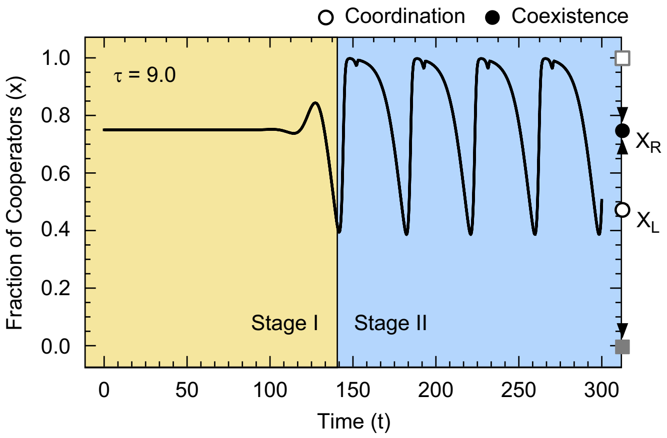

Fig. C.2. Periodic orbits – a different Stage I. We considered a population evolving under a NSH with $\delta = 0.275$ and using a history function with $A = 10^{-10}$ and $B = -1$, instead of the value $B = 1$ used in Figure C.1 Such a variation of the history function with respect to Figure C.1 yields a completely different Stage I.

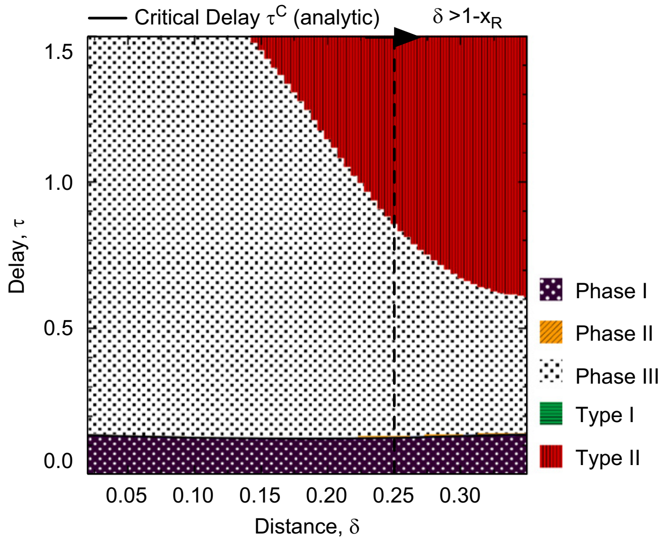

Fig. D.1. Finite size effects in the evolutionary outcome of a population playing a NSH game with an assimetric delay. When only the defectors have delayed fitness, the region of interest is much smaller in τ. For large delays, the population is able to fixate in Full Cooperation through a Type II fixation. We obtain no Type I fixation. The results remain the same for history functions with $B = 1$ and $B = -1$.

ever again reaching this upper bound. However, for different parameters, the population could go over the cut-off in Stage I and afterwards end in Full Defection.

In Fig. C.2 we show how under the same conditions (τ and δ), but for a slight modification of the history function ($B = -1$ instead of $B = 1$), the Stage I is different from that of Fig. C.1, and in particular no Type II fixation occurs. For any pair of values of τ and δ, Type II fixation, because it depends on the transient Stage I, may take place or not depending on the history function. In contrast, Type I fixation is not sensitive to the history function because it depends only on the form of the orbit O, which is completely determined by the parameters τ and δ.

Appendix D. Fixation Types (asymmetric delays)

In this section we present the results of the finite population approach to the asymmetric delay scheme, in complement to those of Section 3.3 of the main text. The notation and definitions are the same of Section 3. The following Fig. D.1 should be compared with Fig. 4 for the infinite population limit, noting that the scale in the τ–axis has been changed to display the region of interest.

Interestingly, the asymmetric delay scheme has no Type I fixation in this parameter region and its fixation behavior is always dependent on the initial conditions. However, we found that Type II fixation is independent of the choice of any of the two history functions that were used.

References

Alboszta, J., Miękisz, J., 2004. Stability of evolutionarily stable strategies in discrete replicator dynamics with time delay. J. Theor. Biol. 231, 175–179.

Freedman, H.L., Rao, V., Sree Hari, 1983. The trade-off between mutual interference and time lags in predator-prey systems. Bull. Math. Biol. 45, 991–1004.

Gyori, I., Ladas, G.E., 1991. Oscillation Theory of Delay Differential Equations: With Applications. Oxford University Press.

Kuang, Y., 1993. Delay Differential Equations: With Aplications in Population Dynamics. Academic Pr.

MacDonald, N., 1978. Time Lags in Biological Models. Springer-Verlag.

McNamara, J.M., Barta, Z., Houston, A.I., 2004. Variation in behaviour promotes cooperation in the Prisoner's dilemma game. Nature 428, 745–748.

Miękisz, J., Wesołowski, S., 2011. Stochasticity and Time delays in evolutionary games. Dyn. Games Appl. 1, 440–448.

Nowak, M.A., May, R.M., 1992. Evolutionary games and spatial chaos. Nature 359, 826–829.

Pacheco, J.M., Pinheiro, F.L., Santos, F.C., 2009a. Population structure induces a symmetry breaking favoring the emergence of cooperation. PLoS comput. biol. 5, e1000596.

Pacheco, J.M., Santos, F.C., Souza, M.O., Skyrms, B., 2009b. Evolutionary dynamics of collective action in n-person stag hunt dilemmas. Proc. R. Soc. B: Biol. Sci. 276, 315.

Pacheco, J.M., Santos, F.C., Souza, M.O., Skyrms, B., 2009c. Evolutionary dynamics of collective action in N-Person stag hunt dilemmas. Proc. Biol. Sci. 276, 315–321.

Perc, M., Szolnoki, A., 2008. Social diversity and promotion of cooperation in the spatial prisoner's dilemma game. Phys. Rev. E 77, 011904.

Santos, F.C., Pacheco, J.M., 2005. Scale-free networks provide a unifying framework for the emergence of cooperation. Phys. Rev. Lett. 95, 98104.

Santos, F.C., Pacheco, J.M., 2011. Risk of collective failure provides an escape from the tragedy of the commons. Proc. Natl. Acad. Sci. USA 108, 10421–10425.

Santos, F.C., Rodrigues, J.F., Pacheco, J.M., 2006. Graph topology plays a determinant role in the evolution of cooperation. Proc. R. Soc. B: Biol. Sci. 273, 51.

Santos, F.C., Santos, M.D., Pacheco, J.M., 2008. Social diversity promotes the emergence of cooperation in public goods games. Nature 454, 213–216.

Santos, F.C., Pinheiro, F.L., Lenaerts, T., Pacheco, J.M., 2011. Role of diversity in the evolution of cooperation. J. Theor. Biol. in press.

Souza, M.O., Pacheco, J.M., Santos, F.C., 2009. Evolution of cooperation under N-person snowdrift games. J. Theor. Biol. 260, 581–588.

Sugden, R., 1986. Economics of Rights Co-operation and Welfare. Oxford.

Szabo, G., Fath, G., 2007. Evolutionary games on graphs. Phys. Rep. 446, 97–216.

Van Segbroeck, S., Santos, F.C., Lenaerts, T., Pacheco, J.M., 2009. Reacting differently to adverse ties promotes cooperation in social networks. Phys. Rev. Lett. 102, 58105.

Yi, T., Zuwang, W., 1997. Effect of time delay and evolutionarily stable strategy. J. Theor. Biol. 187, 111–116.